


## Article

# Improving Thermal Energy Storage in Solar Collectors: A Study of Aluminum Oxide Nanoparticles and Flow Rate Optimization

Mohammad Hamdan <sup>1</sup>, Eman Abdelhafez <sup>2</sup>, Salman Ajib <sup>3,\*</sup> and Mustafa Sukkariyh <sup>2</sup>

<sup>1</sup> Department of Renewable Energy Technology, Faculty of Engineering and Technology, Applied Science Private University, P.O. Box 541350, Amman 11937, Jordan; mo\_ahmad@asu.edu.jo

<sup>2</sup> Department of Alternative Energy Technology, Faculty of Engineering and Technology, Al-Zaytoonah University of Jordan, Amman 11733, Jordan; eman.abdelhafez@zuj.edu.jo (E.A.); m.sukkariyh@zuj.edu.jo (M.S.)

<sup>3</sup> Department of Renewable Energies and Decentralized Energy Supplying, Faculty of Environmental Engineering and Applied Informatics, Technische Hochschule Ostwestfalen-Lippe (University of Applied Sciences and Arts), 32657 Lemgo, Germany

\* Correspondence: salman.ajib@th-owl.de

**Abstract:** Solar thermal energy storage improves the practicality and efficiency of solar systems for space heating by addressing the intermittent nature of solar radiation, leading to enhanced energy utilization, cost reduction, and a more sustainable and environmentally friendly approach to meeting heating needs in residential, commercial, and industrial settings. In this study, an indoor experimental setup was employed to investigate the impact of a water-based Al<sub>2</sub>O<sub>3</sub> nanofluid on the storage capacity of a flat plate solar collector under varying flow rates of the heat transfer fluid. The nanofluid, introduced at specific concentrations, was incorporated into a water-contained storage tank through which the hot heat transfer fluid circulated within a heat exchanger. This process resulted in the storage of thermal energy for future applications. The research identified that the optimal flow rate of the heat transfer fluid, corresponding to the maximum storage temperature, was 15 L per hour, and the ideal nanofluid concentration, associated with the maximum specific heat capacity of the storage medium, was 0.6%. Furthermore, the introduction of nanoparticles into the storage tank led to a significant increase in the specific heat of the water, reaching a maximum of 19% from 4.18 to 5.65 kJ/(kg·°C).

**Keywords:** aluminum oxide nanoparticles; thermal energy storage; solar collectors; improving of system efficiency



**Citation:** Hamdan, M.; Abdelhafez, E.; Ajib, S.; Sukkariyh, M. Improving Thermal Energy Storage in Solar Collectors: A Study of Aluminum Oxide Nanoparticles and Flow Rate Optimization. *Energies* **2024**, *17*, 276. <https://doi.org/10.3390/en17020276>

Academic Editor: Quanqing Yu

Received: 29 November 2023

Revised: 30 December 2023

Accepted: 3 January 2024

Published: 5 January 2024



**Copyright:** © 2024 by the authors. Licensee MDPI, Basel, Switzerland. This article is an open access article distributed under the terms and conditions of the Creative Commons Attribution (CC BY) license (<https://creativecommons.org/licenses/by/4.0/>).

## 1. Introduction

Thermal energy storage plays a crucial role in optimizing energy use, promoting renewable energy integration, enhancing grid stability, and contributing to overall energy efficiency and sustainability. As the world seeks to transition to cleaner and more sustainable energy systems, the importance of thermal energy storage is likely to continue growing. As a result, there has been a growing focus on sustainable and renewable energy sources as a means to mitigate the adverse effects of fossil fuel usage [1–3]. Among these renewable options, solar energy stands out as a highly promising choice due to its numerous advantages, such as its abundance and environmental friendliness [4,5]. One promising approach is the conversion of solar energy into thermal heat, which has the potential to integrate thermal energy storage (TES) with solar thermal collectors. This presents a valuable solution for addressing intermittent solar radiation, whether at night or due to adverse weather conditions. Consequently, TES becomes indispensable, particularly for storing electricity when combined with concentrating solar power (CSP) facilities, where the collected thermal heat can be stored and utilized when solar radiation is unavailable.

The literature presents various techniques employed to enhance the thermal conductivity of TES materials, including methods like bubble agitation [6], encapsulation [7], and the use of extended surfaces and fins [8]. In 1995, the idea of enhancing material properties by introducing tiny solid particles into the mix was explored when Choi proposed improving the thermal conductivity of heat transfer fluids by incorporating nanoparticles (NPs) into the base fluid [9]. An initial investigation into inorganic salt-based nanofluids was conducted by Shin and colleagues in 2010 [10]. In their study, they examined the potential to improve the thermophysical characteristics of the storage medium by dispersing silica NPs into a eutectic salt blend, resulting in nanomaterials. Their findings revealed a significant increase in specific heat capacity as a result of the NP addition. Furthermore, they noted that using these nanomaterials for TES could lead to cost reductions in solar thermal power generation by elevating operating temperatures and reducing material requirements [11,12].

Chavan et al. [13] undertook a research endeavor aimed at establishing a foundational comprehension of the progression of thermal energy storage systems. The assessment of storage system efficacy was conducted through an examination of diverse characterization studies, experimental endeavors, numerical analyses, and patents. The study delved into various techniques implemented to augment thermal performance, providing a thorough review and discussion. The ultimate finding was that composite phase change materials emerged as the most favorable option, striking a balance between cost feasibility and storage capacity in thermal energy storage systems.

Chavan et al. [14] focused on studying a composite phase change material (CPCM) comprising 98% paraffin wax and 2% copper nanoparticle, which was introduced into a confined space. They conducted a numerical analysis to investigate the impact of orientation ( $45^\circ$ ,  $90^\circ$ ,  $135^\circ$ , and  $180^\circ$ ) and varied wall heating conditions (base, left, and top wall) on the flow patterns and interface morphology during the melting/solidification processes. The melting/solidification mechanism displayed non-uniform flow patterns and irregular morphology, influenced by geometric orientations and diverse wall heating conditions. The findings highlighted that the orientation of the confined space significantly affects the formation of natural convection currents. Orientation changes have a substantial impact on the heat transfer rate, leading to an amplification of convection currents. The top wall heating arrangement with a  $180^\circ$  orientation demonstrated effectiveness in achieving superior thermal performance.

Chavan and Guntapure [15] discussed environmental concerns arising from plastic usage and proposed a solution to address these issues by transforming recycled plastics into thermal storage materials (TSM). The impractical thermophysical properties of plastic can be overcome by incorporating additives with superior thermophysical properties, such as functionalized graphene. They concluded that blending recycled plastics with these additives can result in the creation of efficient thermal storage materials.

Chavan et al. [16] concentrated on examining the applications of TES across diverse fields, including waste heat recovery and cooling for heavy electronic equipment. Their extensive investigation revealed that stored thermal energy can be effectively utilized for both heating and cooling purposes, presenting significant potential for the development of innovative technologies and methodologies to maximize its use. Exploring a range of thermal storage materials and methods tailored to different applications offers numerous avenues for advancing sustainable development and optimizing the utilization of existing thermal energy resources.

Numerous research studies have explored the potential improvements in thermophysical properties achieved by incorporating various nanomaterials into different applications, as documented in references [17–19]. Many researchers have specifically focused on the effectiveness of nanofluids/composites in enhancing thermal conductivity, as indicated in references [20–22]. These investigations have consistently demonstrated that adding nanoparticles (NPs) to the base fluid leads to an augmentation in the thermal conductivity of the suspension. This enhancement can be attributed to two primary factors: Brownian

motion (which refers to the random movement of NPs suspended in a fluid due to their collisions with swiftly moving fluid molecules) and the interfacial layer (comprising liquid molecules close to the solid particle surface, forming layered structures) [23–26].

In addition, various researchers have conducted experimental, numerical, and theoretical studies to assess the improvements in conductive and convective heat transfer resulting from the introduction of NPs, Singh et al. [27] conducted simulations work on a parabolic trough collector solar thermal system using nanofluid properties and system advisor model software, showed an enhancement in energy production along with a 10.37% reduction in real power purchase agreement price as well as a 21% reduction in the thermal energy storage volume.

The effect of water-based nanofluids to store the energy and results have been compared with base fluid by studies by Sokhal et al. [28]. It was observed that the nanofluid has more capacity to store energy as compared to the base fluid because of its superior thermal transport properties. The pressure drop is also slightly higher than that of base fluid. The thermal storage capacity of the system is significantly increased when it has been used with nanofluids as compared to base fluids under the same operating conditions.

Yousef et al. [29] reviewed the research development of applying nano-additives to base storage materials. They found that silica and alumina nanoparticles are the most efficient candidates to enhance the specific heat capacity (SHC) of the storage media; using a 1 wt% concentration, an average of up to 120% and 60% enhancement in heat capacity and thermal conductivity/diffusivity, respectively, can be achieved. Furthermore, they showed a significant change in the melting temperature and the heat of fusion for the nano-mixture compared to the base material.

El Far et al. [30] synthesized molten salt nanofluids by dispersing spherical SiO<sub>2</sub> nanoparticles at a minute concentration (1 wt%) into a binary mixture of NaNO<sub>3</sub>-KNO<sub>3</sub>. The results showed that the heat capacity was enhanced by 15% and the viscosity was enhanced by 41–429%.

Alrowaili et al. [31] used mono-CuO and hybrid CuO + Cu/water nanofluids as working fluids to explore the performance of an evacuated tube solar collector. They found that, in the case of the hybrid nanofluid, the thermal conductivity study observed a 21% increase. The performance of the solar PTC collector was tested at flow rates of 0.0125 L/s, 0.015 L/s, and 0.0175 L/s. With the use of a hybrid nanofluid, the collector area can be reduced by up to 38%. The heat removal factor was found to be 0.894. The hybrid CuO 2.5 g + Cu 1.5 g nanofluid exhibited 61.7% and 14.9% greater thermal-optical efficiency than water and mono-CuO, respectively.

Alamayreh and Alahmar [32] used a solar-thermal hybrid system that utilizes a parabolic solar dish (PSD) with a cylindrical solar receiver to capture both heat and solar radiation. The system involves transmitting light to internal photovoltaic panels through fiber optics, serving as an illumination source for the building while concurrently generating hot household water. In their experimental approach, they incorporated a direct storage system with phase change material (PCM) using petroleum jelly to prolong the duration of water heating. To enhance heat transfer during heat charge and discharge, 1% of Al<sub>2</sub>O<sub>3</sub> nanoparticles were added to the PCM material. Additionally, a low-cost, two-axis tracking system for the PSD was developed. The experimental results demonstrated a 5.68% increase in thermal efficiency with the incorporation of Al<sub>2</sub>O<sub>3</sub> nanoparticles.

As mentioned earlier, prior research focused on improving thermal solar energy storage through nanotechnology. This involved introducing nanoparticles either into the heat transfer fluid within the collector [31] or incorporating them into phase change materials [7]. To the authors' knowledge, no prior studies have explored the incorporation of Al<sub>2</sub>O<sub>3</sub> nanoparticles into a water-contained storage tank. This serves as the motivation for the current research.

In this study, we utilized an indoor thermal energy storage system acquired from Gunt, Hamburg, to investigate the impact of incorporating Al<sub>2</sub>O<sub>3</sub> nanoparticles on the storage capacity of water within a storage tank. The water volume in the tank undergoes

heating as the heat transfer fluid exits the flat plate solar collector and travels through a heat exchanger integrated with the storage tank. Subsequently, the heated heat transfer fluid is returned to the collector for reheating.

## 2. Theoretical Analysis

The equation representing the output energy from the solar thermal collector within the solar thermal energy simulator and subsequently transferred to the heat exchanger integrated with the storage system ( $\dot{Q}_{exchanger}$ ) is expressed as follows:

$$\dot{Q}_{exchanger} = \dot{m}_{exchanger} * C_p * (T_2 - T_1) * \text{Time} \quad (1)$$

where the mass flow rate of the heat exchanger ( $\dot{m}_{exchanger}$ ) can be found using the following equation:

$$\dot{m}_{exchanger} = \text{Flow Rate} * \text{Density} \quad (2)$$

The thermal energy stored in the tank can be determined using the following equation:

$$\dot{Q}_{tank} = m_{tank} * C_p * (T_{3,final} - T_{3,intial}) \quad (3)$$

where the mass of the liquid in the tank can be determined using the following:

$$m_{tank} = \text{Volume} * \text{Density} \quad (4)$$

Following the first law of thermodynamics, which asserts the conservation of energy, stipulating that energy cannot be created nor destroyed but only transformed from one form to another, the energy output from the heat exchanger is equivalent to the energy input into the tank.

$$\dot{Q}_{exchanger} = \dot{Q}_{tank} \quad (5)$$

By applying Equations (1) through (5), the heat capacity of the working fluid within the tank can be calculated as follows:

$$C_p = \frac{\dot{Q}_{exchanger}}{m_{tank} * (T_{3,final} - T_{3,intial})} \quad (6)$$

Ultimately, the overall efficiency of the system ( $\eta_{all}$ ) is

$$\eta_{all} = \eta_0 - \frac{k_1 * \Delta T}{\text{Solar Radiation}} - \frac{k_2 * \Delta T^2}{\text{Solar Radiation}} \quad (7)$$

where  $\eta_0$  is the optical efficiencies,  $k_1$  denotes the linear loss coefficient (unit: W/m<sup>2</sup>K),  $k_2$  is the quadratic loss coefficient (unit: W/m<sup>2</sup>K<sup>2</sup>), and  $\Delta T$  is the temperature difference between collector and environment.

## 3. Materials and Methods

### 3.1. Selection of Materials

Aluminum oxide nanoparticles, also referred to as alumina nanoparticles, find frequent application in photovoltaic (PV) cooling due to their distinct properties and advantages. The utilization of these nanoparticles is widespread in PV cooling applications because of their noteworthy characteristics such as high thermal conductivity, a substantial surface area, stability, compatibility, cost-effectiveness, and ease of integration. The prevalence of aluminum oxide nanoparticles in PV cooling is attributed to their ability to efficiently dissipate heat, thus playing a pivotal role in upholding the efficacy and durability of PV systems [33]. In this study, Al<sub>2</sub>O<sub>3</sub> nanofluids with particles sized at approximately 30 nm were purchased from US Research Nanomaterials, Inc., Houston, TX, USA.

### 3.2. Test Method

Figure 1 depicts the essential components of the experimental arrangement utilized in this study. The primary apparatus employed is the ET 202: Principles of Solar Thermal Energy, procured from Gunt, Hamburg. The lighting unit (1) is equipped with 25 halogen lamps. Halogen lamps are occasionally employed in scientific and industrial environments to provide simulated sunlight for experiments and testing. Although they do not serve as a substitute for authentic solar radiation, they were utilized in this study to control certain variables like light intensity, spectrum, and exposure duration parameters that might be challenging to achieve with natural sunlight. Additionally, halogen lamps provide a more reliable and reproducible light source, enabling researchers to conduct experiments under stable and predetermined conditions. This illumination permeates the flat plate collector (2), causing the absorber within it to heat up. The absorber transfers heat to the circulating heat transfer fluid, which then exits the flat plate collector and enters the tank (3).

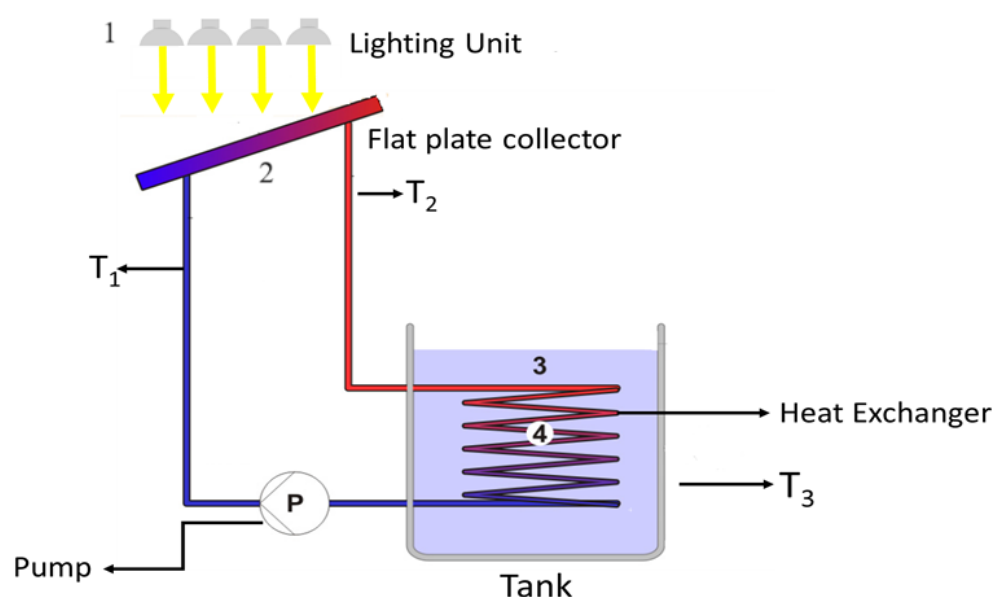


Figure 1. Experiment setup.

A pipe integrated into the solar circuit within the flat plate collector facilitates the circulation of the heat transfer fluid (water) using a pump (P). The pump can adjust the flow rate of the heat transfer fluid within the range of 5 to 30 L per hour. Through experimentation in this study, the optimal mass flow rate was determined to be 15 L per hour, achieved with a pump input power of 20 W. It is important to highlight that this input power corresponds to 9.7% of the total collected solar radiation power controlled by the pump. Accurate measurement of the heat transfer fluid's flow rate is essential for calculating the produced heat quantity.

The tank's pipe is configured in a spiral shape, functioning as a heat exchanger (4). As a result, the water in the tank heats up while the heat transfer fluid cools down. The pump then propels the cooled heat transfer fluid back to the flat plate collector, establishing a closed solar circuit. The solar circuit incorporates a ventilator and an overflow, with the overflow compensating for volume expansions in the heat transfer fluid. Temperature measurements at critical points are conducted using sensors.

The temperature of the heat transfer fluid is monitored at both the collector inlet (flowing into the collector) and outlet (returning from the collector) using temperature sensors  $T_1$  and  $T_2$ . This allows for the measurement of the temperature rise achieved within the collector. The heat transfer fluid is introduced into the heat exchanger through the solar circuit, leading to an increase in the temperature of the tank contents. Temperature sensor  $T_3$  is employed to ascertain the temperature of the tank contents, and it is positioned at the midpoint of the tank's height.

To analyze the measurement results, it is essential to determine the temperature of the surrounding air. Temperature sensor  $T_4$ , integrated into the control cabinet of the trainer, is responsible for detecting this ambient air temperature. Positioned at the side, near the system diagram and adjacent to the USB port, the sensor provides this crucial temperature data.

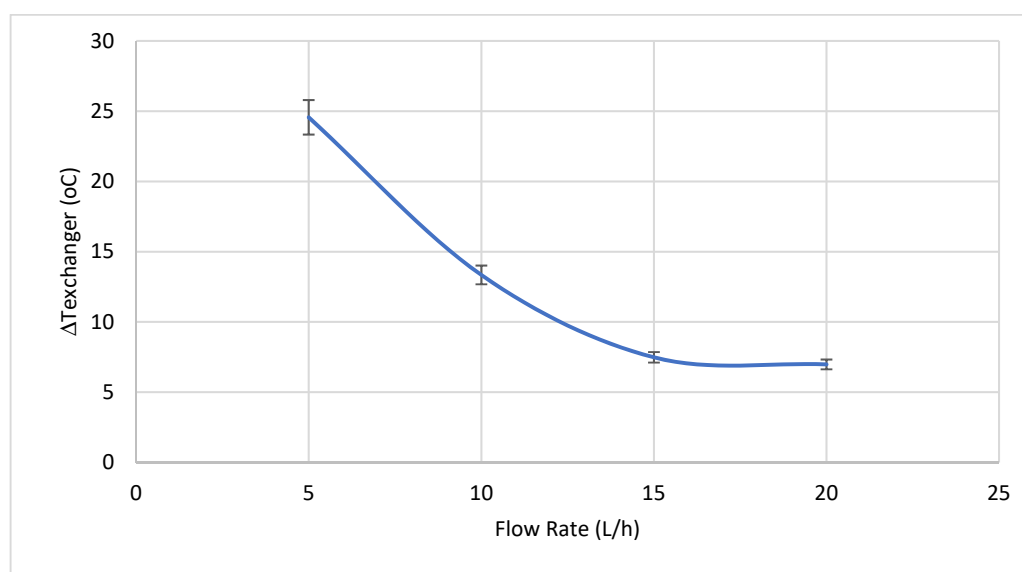
As a first step, the optimum flow rate that corresponds to the best performance of the system, which is indicated by the maximum storage temperature, was estimated. This was accomplished by measuring the average storage temperature that corresponds to a certain flow rate of the heat transfer fluid, which indicated the pump speed. The second step of the work was conducted with the heat transfer fluid being fixed at the optimal value. Nanoparticles were added at different concentrations to the water-contained tank, and the effect of this addition on the storage capacity of the system was determined by the measurement of the collector outlet and inlet temperatures, the average storage tank temperature, using copper constant thermocouples, which are connected to a data logger. These measured temperature values were used to estimate the storage capacity of the system at various values of nanoparticle concentrations.

In this study, it was assumed that the heat lost from the heat transfer fluid as it flows within the exchanger is the same that was gained by the water in the storage tank. Based on this, the specific heat of storage water was easily calculated.

#### 4. Results and Discussions

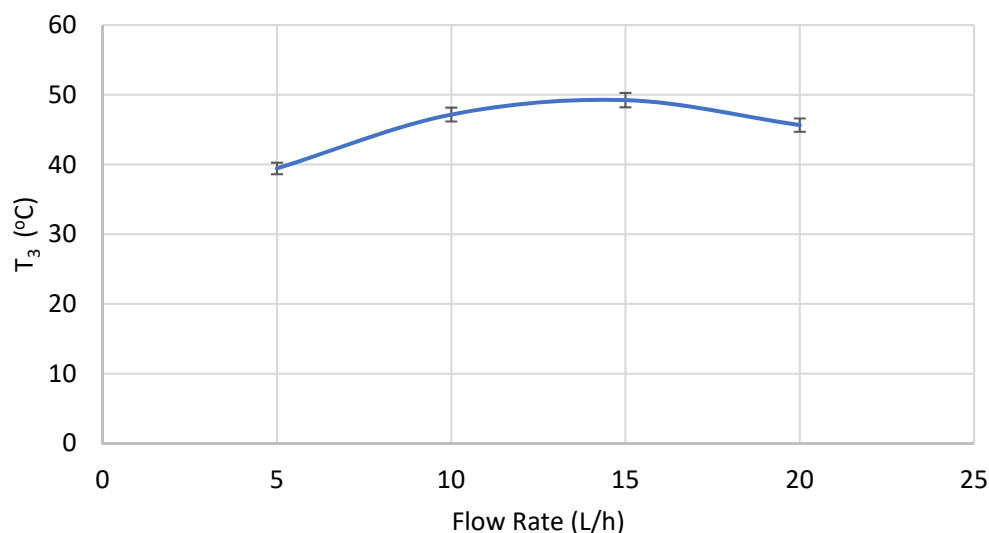
In this section, we explore the core of our research discoveries and the methodical procedures that directed our inquiry. The outcomes offer a thorough view of our study's results, providing perspectives on the observed patterns, trends, and implications. While navigating the complexities of our data, our goal is to clarify the importance of our findings within the framework of the research questions raised.

Figure 2 represents the temperature drop of the heat transfer fluid as it flows inside the heat exchanger. As it may be noticed, this temperature drop decreases with the flow rate, which may be attributed to the fact that the residence time of the fluids within the heat exchanger decreases, and hence the fluids have less time to exchange heat, resulting in a smaller temperature drop. Furthermore, higher flow rates can promote turbulence and improve heat transfer efficiency. This can result in a higher heat transfer coefficient, allowing for more effective heat loss from the heat transfer fluid. With increased heat transfer, the temperature difference between the inlet and outlet may decrease.



**Figure 2.** The temperature drops of the heat transfer fluid along the heat exchanger on the mass flow rate.

Figure 3 shows the variation in the average temperature of the storage tank with the flow rate of the heat transfer fluid. As indicated, the temperature increases with the flow rate up to a certain flow rate value, beyond which the temperature starts to decrease. The initial increase in the temperature is a result of the heat gained by the water in the storage tank. However, as the flow rate increases beyond 15 L/h, the temperature decreases. This is due to the fact that the residence time of the fluid decreases, and hence less heat is gained by the water in the tank, which leads to a decrease in the storage temperature.



**Figure 3.** Variation in the storage temperature with the mass flow rate of the heat transfer fluid.

As presented in Figure 4, the efficiency of a thermal energy system can be influenced by the flow rate of the heat transfer fluid, as the heat that flows into the storage tank increases with the flow rate of the heat transfer fluid, which contains high thermal energy; consequently, the efficiency of the storage system increases. Furthermore, higher flow rates can enhance heat transfer in some systems. This is because a faster-moving fluid can promote turbulence and improve the overall heat transfer coefficient. In such cases, an increase in flow rate may lead to higher efficiency by allowing for a more effective transfer of thermal energy. However, as the flow rate of the heat transfer fluid increases, the efficiency of the system decreases, since higher flow rates can result in reduced residence time of the heat transfer fluid within the heat exchanger. This means that the fluid has less time to exchange heat with the storage material. As a result, the thermal storage system may not be able to absorb or release heat effectively, leading to lower overall efficiency.

Figure 5 illustrates the average specific heat capacity ( $C_p$ ) for the different nanoparticle concentrations in the nanofluid compared to the baseline water. It is evident that the introduction of nanoparticles has a notable impact on the thermal characteristics of the nanofluid, with all modified nanofluids exhibiting higher  $C_p$  values than pure water. The most striking observation is associated with the nanofluid containing a 0.6% concentration of water-based  $Al_2O_3$  nanoparticles. This particular nanofluid surpasses the  $C_p$  of water by a substantial 23.5%, indicating a significant enhancement in its heat storage and transfer capabilities. As shown in the figure, the maximum  $C_p$  observed at 0.6% nanoparticle concentration implies an optimal point, where the enhancements in thermal properties are most pronounced. Beyond this concentration, there appears to be a slight decline in  $C_p$ , indicating potential saturation or interparticle interaction effects influencing the thermal response of the nanofluid.

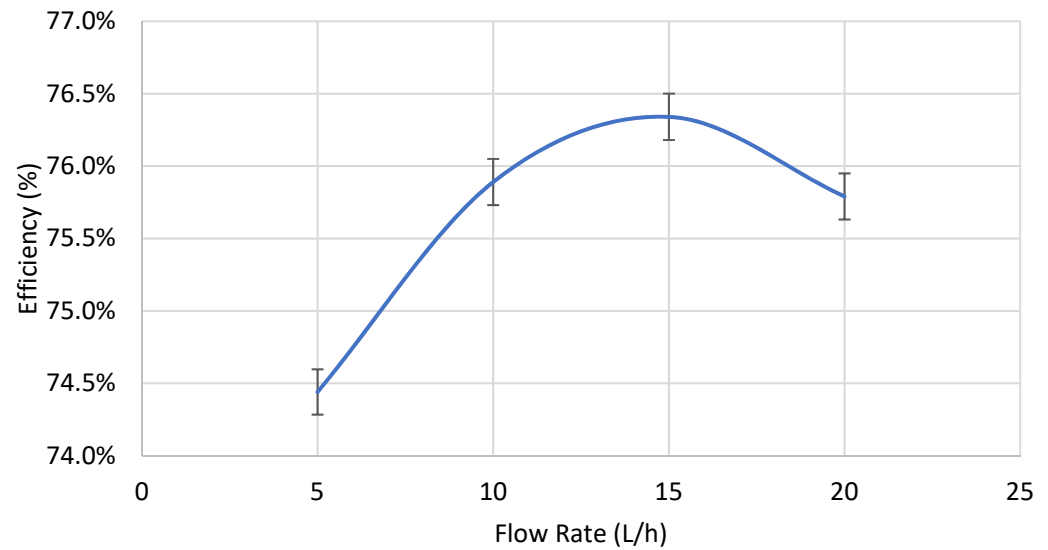


**Figure 4.** Variation in the storage system efficiency with the mass flow rate of the heat transfer fluid.

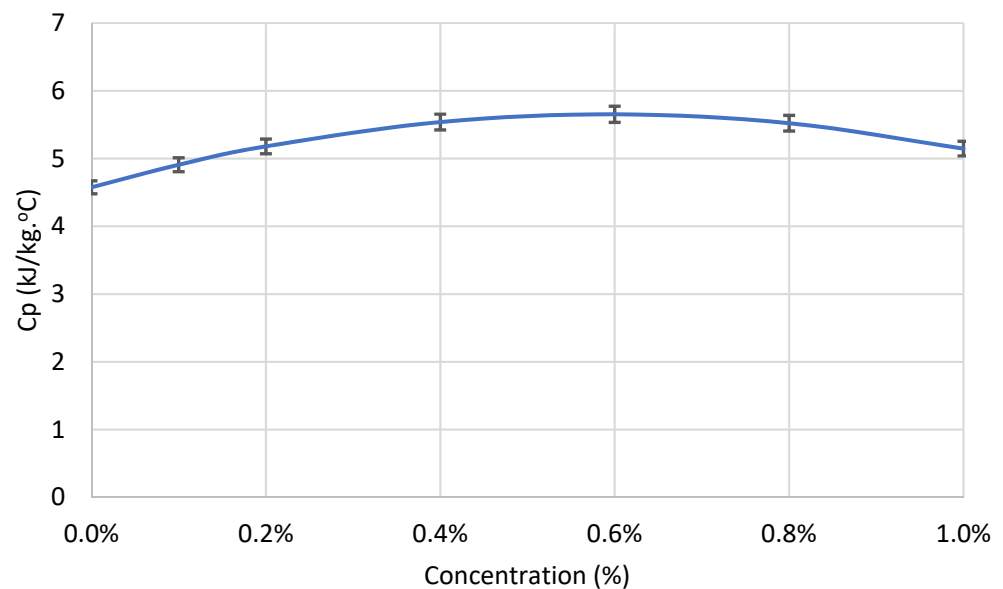


**Figure 5.** The variation in the average heat capacity with the concentration of nanoparticles.

In Figure 6, the average temperature profiles of the storage tank for different concentrations of water-based  $\text{Al}_2\text{O}_3$  nanoparticles are presented. A noteworthy trend emerges, revealing that all modified nanofluids consistently exhibit lower temperatures compared to the baseline water. The most striking observation pertains to the nanofluid with a 0.6% concentration of nanoparticles, which demonstrates the lowest temperature among all concentrations. Surpassing the water temperature by 2.9%, this finding implies an efficient cooling effect associated with the introduction of nanoparticles into the fluid. The maximum cooling effect observed at a 0.6% nanoparticle concentration suggests an optimal point where the thermal characteristics of the nanofluid are most pronounced. Beyond this concentration, there is a slight deviation from the cooling trend, indicating potential saturation or interaction effects that warrant closer examination.



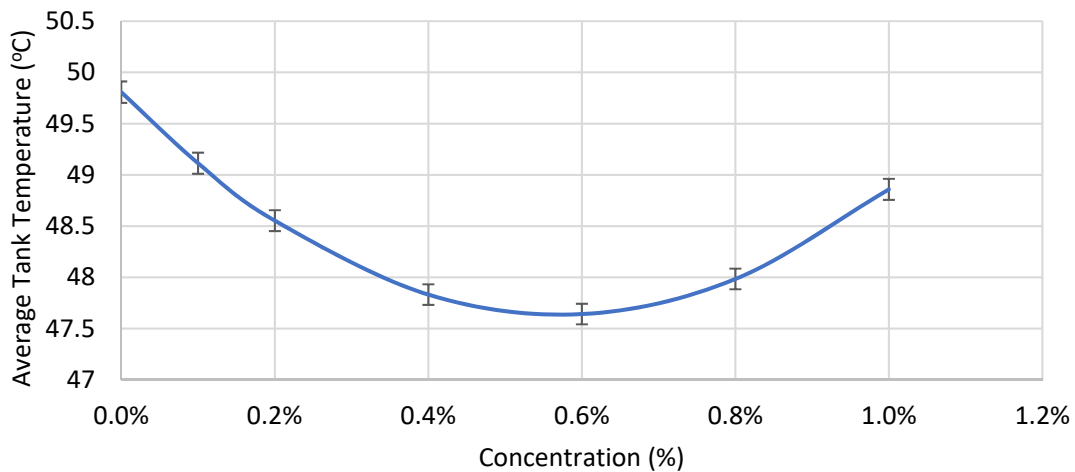


**Figure 6.** The variation in the average tank temperature with the concentration of nanoparticles.

The initial decline in tank temperature as the flow rate increases can be explained by the introduction of nanoparticles into the tank, which tends to raise the thermal conductivity of the water. This, in turn, enhances heat loss from the tank, resulting in a decrease in temperature. However, as the nanoparticle concentration rises, there is a likelihood of nanoparticle agglomeration, causing a reduction in heat loss from the tank due to the increased thermal conductivity of the water inside the tank, and hence the tank temperature increases.

Figure 7 demonstrates the impact of nanoparticle concentration on thermal storage efficiency. As depicted in the figure, there is an initial decline in system efficiency with the increasing nanoparticle concentration. However, beyond a concentration of 0.6%, efficiency begins to rise. This fluctuation in efficiency is attributed to changes in thermal conductivity resulting from the addition of nanoparticles. The initial increase in the thermal conductivity of the storage water contributes to greater heat loss and, consequently, a decrease in system efficiency. Conversely, higher nanoparticle concentrations lead to increased efficiency due to reduced thermal conductivity resulting from nanoparticle agglomeration.

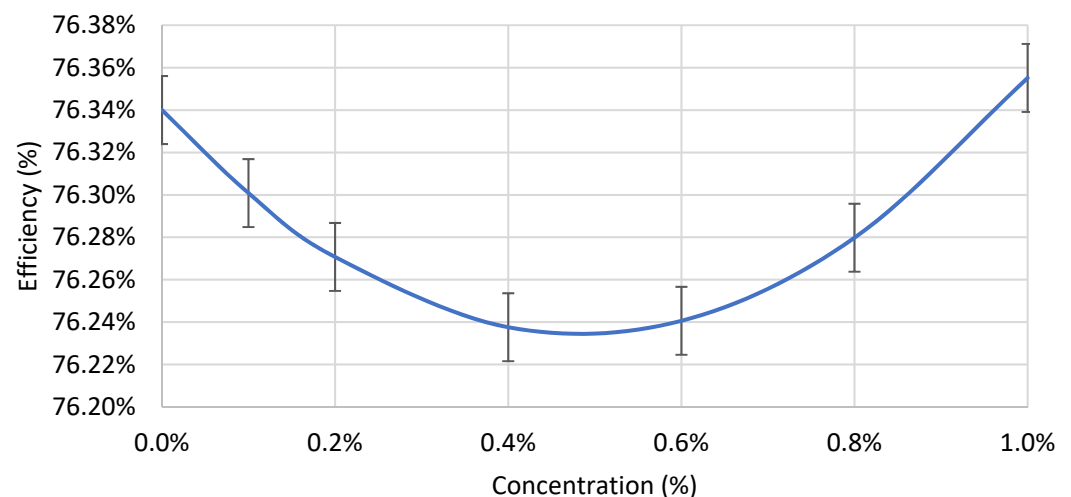


**Figure 7.** The variation in the storage system efficiency with the concentration of nanoparticles.

## 5. Uncertainty Analysis

Uncertainty is characterized by the inherent limitations of several measurement components. It arises from various factors such as measurement techniques, instruments, operators, and the ambient conditions. Analyzing uncertainty is essential to evaluate the accuracy of measurement results. This process ensures the validation of data integrity, and a

comprehensive method for precisely calculating uncertainty is presented. Equation (8) illustrates the uncertainties stemming from the computation ( $U_R$ ) due to multiple independent variables [34].

$$U_R = \left[ \left( \frac{\partial R}{\partial x_1} u_1 \right)^2 + \left( \frac{\partial R}{\partial x_2} u_2 \right)^2 + \cdots + \left( \frac{\partial R}{\partial x_n} u_n \right)^2 \right]^{1/2} \quad (8)$$

where the result  $R$  is a function in terms of its independent variables as  $x_1, x_2, \dots, x_n$ ; thus,  $R = R(x_1, x_2, \dots, x_n), u_1, u_2, \dots, u_n$  are the uncertainties in the independent variables and  $U_R$  is the uncertainty of the result.

After applying Equation (8), the overall accuracy of the system is  $\pm 2.1\%$ , according to the data.

## 6. Conclusions

In this work, the effect of  $Al_2O_3$  nanoparticles on the performance of a thermal energy storage system was successfully achieved using an indoor setup at different flow rates of the thermal heat fluid. The incorporation of nanoparticles into a solar thermal energy storage system has a notable impact on its performance. Initially, the addition of nanoparticles tends to enhance the thermal conductivity of the storage medium, which is typically water. This heightened thermal conductivity results in increased heat loss from the system, leading to an initial decrease in overall efficiency. However, as the concentration of nanoparticles surpasses a certain threshold, a phenomenon of agglomeration occurs. This agglomeration causes a reduction in thermal conductivity, mitigating heat loss and subsequently improving the efficiency of the solar thermal energy storage system. Therefore, the careful manipulation of nanoparticle concentration becomes a critical factor in optimizing the balance between enhanced thermal properties and efficient energy storage in solar systems.

From this study, the following may be concluded:

- The optimal flow rate of the heat transfer fluid, corresponding to the maximum storage temperature, was 15 L per hour.
- The ideal nanofluid concentration, associated with the maximum specific heat capacity of the storage medium, was 0.6%.
- The introduction of nanoparticles into the storage tank led to a significant increase in the specific heat of water, reaching a maximum of 19% from 4.18 to 5.65 kJ/(kg·°C).
- The optimal nanofluid concentration, associated with the maximum storage system efficiency, was 1.0%.

**Author Contributions:** Conceptualization, M.H. and S.A.; Methodology, E.A. and S.A.; Validation, E.A. and M.S.; Formal analysis, E.A.; Investigation, E.A. and M.S.; Data curation, M.S.; Writing—original draft, M.H. and E.A.; Writing—review & editing, S.A.; Supervision, M.H. All authors have read and agreed to the published version of the manuscript.

**Funding:** This research received no external funding.

**Data Availability Statement:** Data are contained within the article.

**Conflicts of Interest:** The authors declare no conflict of interest.

## References

1. Elsaid, K.; Sayed, E.T.; Abdelkareem, M.A.; Baroutaji, A.; Olabi, A.G. Environmental Impact of Desalination Processes: Mitigation and Control Strategies. *Sci. Total Environ.* **2020**, *740*, 140125. [[CrossRef](#)] [[PubMed](#)]
2. Elsaid, K.; Sayed, E.T.; Abdelkareem, M.A.; Mahmoud, M.S.; Ramadan, M.; Olabi, A.G. Environmental Impact of Emerging Desalination Technologies: A Preliminary Evaluation. *J. Environ. Chem. Eng.* **2020**, *8*, 104099. [[CrossRef](#)]
3. Elsaid, K.; Taha Sayed, E.; Yousef, B.A.A.; Kamal Hussien Rabaia, M.; Ali Abdelkareem, M.; Olabi, A.G. Recent Progress on the Utilization of Waste Heat for Desalination: A Review. *Energy Convers. Manag.* **2020**, *221*, 113105. [[CrossRef](#)]

4. Sivaram, P.M.; Mande, A.B.; Premalatha, M.; Arunagiri, A. Investigation on a Building-Integrated Passive Solar Energy Technology for Air Ventilation, Clean Water and Power. *Energy Convers. Manag.* **2020**, *211*, 112739. [[CrossRef](#)]
5. Karaca, A.E.; Dincer, I. A New Integrated Solar Energy Based System for Residential Houses. *Energy Convers. Manag.* **2020**, *221*, 113112. [[CrossRef](#)]
6. Shah, Y.T. *Thermal Energy: Sources, Recovery, and Applications*; Boca Raton Crc Press, Taylor & Francis Group: Boca Raton, FL, USA, 2018.
7. Sarbu, I.; Dorca, A. Review on Heat Transfer Analysis in Thermal Energy Storage Using Latent Heat Storage Systems and Phase Change Materials. *Int. J. Energy Res.* **2018**, *43*, 29–64. [[CrossRef](#)]
8. Gasia, J.; Miró, L.; Cabeza, L.F. Materials and System Requirements of High Temperature Thermal Energy Storage Systems: A Review. Part 2: Thermal Conductivity Enhancement Techniques. *Renew. Sustain. Energy Rev.* **2016**, *60*, 1584–1601. [[CrossRef](#)]
9. Zhao, C.Y.; Wu, Z.G. Heat Transfer Enhancement of High Temperature Thermal Energy Storage Using Metal Foams and Expanded Graphite. *Sol. Energy Mater. Sol. Cells* **2011**, *95*, 636–643. [[CrossRef](#)]
10. Choi, S.U.; Eastman, J.A. *Enhancing Thermal Conductivity of Fluids with Nanoparticles*; Argonne National Laboratory: Argonne, IL, USA, 1995.
11. Al-Kayiem, H.; Lin, S.; Lukmon, A. Review on Nanomaterials for Thermal Energy Storage Technologies. *Nanosci. Nanotechnol.-Asia* **2013**, *3*, 60–71. [[CrossRef](#)]
12. Shin, D.; Banerjee, D. Effects of Silica Nanoparticles on Enhancing the Specific Heat Capacity of Carbonate Salt Eutectic (Work in Progress). *Int. J. Struct. Chang. Solids* **2010**, *2*, 25–31.
13. Chavan, S.; Gumtapure, V.; Perumal, D.A. A review on thermal energy storage using composite phase change materials. *Recent Pat. Mech. Eng.* **2018**, *11*, 298–310. [[CrossRef](#)]
14. Chavan, S.; Gumtapure, V.; Perumal, D.A. Computational investigation of bounded domain with different orientations using CPCM. *J. Energy Storage* **2019**, *22*, 355–372. [[CrossRef](#)]
15. Chavan, S.; Gumtapure, V. Numerical and experimental analysis on thermal energy storage of polyethylene/functionalized graphene composite phase change materials. *J. Energy Storage* **2020**, *27*, 101045. [[CrossRef](#)]
16. Chavan, S.; Rudrapati, R.; Manickam, S. A comprehensive review on current advances of thermal energy storage and its applications. *Alex. Eng. J.* **2022**, *61*, 5455–5463. [[CrossRef](#)]
17. Wang, X.; Mujumdar, A.S. Heat Transfer Characteristics of Nanofluids: A Review. *Int. J. Therm. Sci.* **2007**, *46*, 1–19. [[CrossRef](#)]
18. Wang, X.; Mujumdar, A.S. A Review on Nanofluids—Part II: Experiments and Applications. *Braz. J. Chem. Eng.* **2008**, *25*, 631–648. [[CrossRef](#)]
19. Ali, A.H.; Ibrahim, S.I.; Jawad, Q.A.; Jawad, R.S.; Chaichan, M.T. Effect of Nanomaterial Addition on the Thermophysical Properties of Iraqi Paraffin Wax. *Case Stud. Therm. Eng.* **2019**, *15*, 100537. [[CrossRef](#)]
20. Qiu, L.; Zhu, N.; Feng, Y.; Michaelides, E.E.; Żyła, G.; Jing, D.; Zhang, X.; Norris, P.M.; Markides, C.N.; Mahian, O. A Review of Recent Advances in Thermophysical Properties at the Nanoscale: From Solid State to Colloids. *Phys. Rep.* **2020**, *843*, 1–81. [[CrossRef](#)]
21. Fan, J.; Wang, L. Effective Thermal Conductivity of Nanofluids: The Effects of Microstructure. *J. Phys. D* **2010**, *43*, 165501. [[CrossRef](#)]
22. Mahian, O.; Kianifar, A.; Kalogirou, S.A.; Pop, I.; Wongwises, S. A Review of the Applications of Nanofluids in Solar Energy. *Int. J. Heat Mass Transf.* **2013**, *57*, 582–594. [[CrossRef](#)]
23. Zhai, S.; Zhang, P.; Xian, Y.; Yuan, P.; Yang, D. Modelling and Analysis of Effective Thermal Conductivity for Polymer Composites with Sheet-like Nanoparticles. *J. Mater. Sci.* **2018**, *54*, 356–369. [[CrossRef](#)]
24. Nasiri, A.; Shariaty-Niasar, M.; Rashidi, A.M.; Khodafarin, R. Effect of CNT Structures on Thermal Conductivity and Stability of Nanofluid. *Int. J. Heat Mass Transf.* **2012**, *55*, 1529–1535. [[CrossRef](#)]
25. Gupta, M.; Singh, V.; Kumar, R.; Said, Z. A Review on Thermophysical Properties of Nanofluids and Heat Transfer Applications. *Renew. Sustain. Energy Rev.* **2017**, *74*, 638–670. [[CrossRef](#)]
26. Xuan, Y.; Li, Q. Heat Transfer Enhancement of Nanofluids. *Int. J. Heat Fluid Flow* **2000**, *21*, 58–64. [[CrossRef](#)]
27. Singh, T.; Almanassra, I.W.; Ghani Olabi, A.; Al-Ansari, T.; McKay, G.; Ali Atieh, M. Performance Investigation of Multiwall Carbon Nanotubes Based Water/Oil Nanofluids for High Pressure and High Temperature Solar Thermal Technologies for Sustainable Energy Systems. *Energy Convers. Manag.* **2020**, *225*, 113453. [[CrossRef](#)]
28. Sokhal, G.S.; Dhindsa, G.S.; Malhi, G.S. Performance of Thermal Storage System with Water Based Nanofluids. *Mater. Today Proc.* **2022**, *48*, 1502–1507. [[CrossRef](#)]
29. Yousef, B.A.A.; Elsaid, K.; Abdelkareem, M.A. Potential of Nanoparticles in Solar Thermal Energy Storage. *Therm. Sci. Eng. Prog.* **2021**, *25*, 101003. [[CrossRef](#)]
30. El Far, B.; Rizvi, S.M.M.; Nayfeh, Y.; Shin, D. Study of Viscosity and Heat Capacity Characteristics of Molten Salt Nanofluids for Thermal Energy Storage. *Sol. Energy Mater. Sol. Cells* **2020**, *210*, 110503. [[CrossRef](#)]
31. Alrowaili, Z.A.; Ezzeldien, M.; Shaaalan, N.M.; Hussein, E.; Sharafeldin, M.A. Investigation of the Effect of Hybrid CuO-Cu/Water Nanofluid on the Solar Thermal Energy Storage System. *J. Energy Storage* **2022**, *50*, 104675. [[CrossRef](#)]
32. Alamayreh, M.I.; Alahmer, A. Design a solar harvester system capturing light and thermal energy coupled with a novel direct thermal energy storage and nanoparticles. *Int. J. Thermofluids* **2023**, *18*, 100328. [[CrossRef](#)]

33. Sutanto, B.; Indartono, Y.S. Numerical approach of Al<sub>2</sub>O<sub>3</sub>-water nanofluid in photovoltaic cooling system using mixture multiphase model. *IOP Conf. Ser. Earth Environ. Sci.* **2018**, *168*, 012003. [[CrossRef](#)]
34. Basri, M.; Haddada, J.; Tarakka, R.; Syahid, M.; Ramadhani, M.A. Experimental study of modified absorber plate integrated with aluminium foam of solar water heating system. *Int. J. Renew. Energy Res.* **2022**, *12*, 993–999. [[CrossRef](#)]

**Disclaimer/Publisher’s Note:** The statements, opinions and data contained in all publications are solely those of the individual author(s) and contributor(s) and not of MDPI and/or the editor(s). MDPI and/or the editor(s) disclaim responsibility for any injury to people or property resulting from any ideas, methods, instructions or products referred to in the content.